Journal of Thermal Analysis and Calorimetry, Vol. 79 (2005) 439–443

DETERMINATION OF SURFACE PROPERTIES OF NICKEL SUPPORTED ON HY ZEOLITE BY TG, DTA AND TPR

A. M. Garrido Pedrosa[1*], *M. J. B. Souza*[2], *D. M. A. Melo*[1], *A. G. Souza*[3] *and A. S. Araujo*[1]

[1]Federal University of Rio Grande do Norte, Department of Chemistry, CP 1662, 59078-970 Natal, RN, Brazil
[2]Federal University of Rio Grande do Norte, Department of Chemical Engineering, CP 1662, 59078-970 Natal, RN, Brazil
[3]Federal University of the Paraíba, CCEN, Department of Chemistry, 59059-900 João Pessoa, PB, Brazil

In this work the properties of HY zeolite containing nickel oxide was investigated using thermal analysis (TG/DTA) and temperature-programmed reduction (TPR). The results obtained by XRD and FTIR showed that the impregnation method used did not change the structure of HY zeolite. TPR profiles showed two events at 238 and 507°C which were attributed to reduction of nickel oxide on the HY cavities at different temperatures. The thermodesorption of *n*-butylamine from Ni*/HY zeolite showed typically two larger mass loss events attributed to the elimination of *n*-butylamine adsorbed on the weak acid sites and on the medium+strong acid sites.

Keywords: *DTA, HY zeolite, nickel, TG, TPR*

Introduction

Bifunctional catalysts contain platinum, palladium or nickel supported on zeolites can be used in several hydrocarbon reactions as hydroisomerization, hydrocracking, hydrogenation among other reactions [1, 2]. The activity and selectivity of these bifunctional catalysts for such hydrocarbon reactions depend on the characteristics of the acidic and metallic sites [3] where the acidity and pore structure of the acid support influence mainly the selectivity [4]. Y zeolite with or without incorporated metals have been studied for such process due its large three-dimensional pore system [5]. Y zeolite is a synthetic molecular sieve with three-dimensional 12-membered-ring pore system. This pore system consists of spherical cages, referred to as super cages with a diameter of 1.3 nm connected of tetrahedral shape with four neighboring cages through windows with a 0.74 nm diameter [6].

The acid properties of bifunctional catalysts have been studied in the literature for several techniques such as TPD, TG and FTIR. Thermal analysis has been applied to study the acid properties of zeolite catalysts from thermodesorption of bases adsorbed [7–9]. On the other hand, the metallic properties of bifunctional catalysts have been studied by TPR (reduction by programmed temperature) [10, 11]. In this analysis the supported metal oxide is reduced by mixture of hydrogen and some inert gases such as argon, nitrogen or helium. The reduction of metallic ion supported in zeolites depends basically on its potential of reduction and its interaction with the supporter [10, 12, 13]. In this work we have synthetized a bifunctional catalyst of nickel supported on HY zeolite and studied their acid and metallic properties by TG/DTA and TPR techniques. XRD and FTIR techniques were used to investigate structural properties of the catalysts.

Experimental

The NaY zeolite was supplied by Union Carbide Corporation with an atomic ratio of Si/Al=2.36 and was highly crystalline. The acid form of this zeolite was obtained by ion exchange with 1 M NH_4Cl solution at 70°C for 2 h. After, this material was filtered, dried and calcined in air atmosphere at 500°C for 4 h resulting in the acid form (HY). The supported metallic catalyst was prepared by incipient wetness impregnation using 1 mass% metal from $Ni(NO_3)_2{\cdot}6H_2O$ solution and subsequent calcination in air atmosphere at 500°C for 1 h. The NaY, HY and Ni*/HY zeolites (Ni*=nickel oxides) were characterized by atomic absorption (Varian AA-175), X-ray diffraction (Shimadzu XRD-6000), Fourier-transform infrared spectroscopy (ABB Bomem MB104) and nitrogen adsorption (Quanta Chrome NOVA 2000). Thermoanalytical measurements were carried out on a Perkin Elmer TGA-7 instrument and on a Perkin Elmer DTA-1700 instrument at a heating rate of 10°C min^{-1} in dynamic air flow at a rate of 50 cm^3 min^{-1}. The acid properties of the HY and Ni*/HY zeolites were investigated by *n*-butylamine desorption. The procedure con-

* Author for correspondence: annemgp@yahoo.com

1388–6150/$20.00

Akadémiai Kiadó, Budapest, Hungary
Springer, Dordrecht, The Netherlands

Table 1 Compositional and textural characteristics of NaY, HY and Ni*/HY zeolite samples

Samples	Unit cell composition	Ni/%	BET surface area/m^2 g^{-1}	Micropore area/m^2 g^{-1}
NaY	$Na_{57.2}Al_{58.2}Si_{133.8}O_{384}$	–	498.4	491.9
HY	$Na_{10.9}H_{46.3}Al_{54.8}Si_{137.2}O_{384}$	–	312.3	307.7
Ni*/HY	$Na_{10.6}H_{46.1}Al_{54.5}Si_{137.4}O_{384}$	1.1	237.9	219.0

sisted of activating the sample at 400°C for 30 min in nitrogen flow. After that the temperature was decreased to 95°C and the sample was saturated with *n*-butylamine vapors for 30 min. The sample was saturated with amine and purged with nitrogen for 30 min at the same adsorption temperature to remove the physically adsorbed base. The *n*-butylamine desorption was performed by heating of 10 mg of saturated sample using a Mettler TGA-851 instrument at a heating rate of 20°C min^{-1} and under nitrogen flow at a rate of 25 cm^3 min^{-1}. The bifunctional catalyst was characterized by temperature programmed reduction (TPR). TPR experiments had been carried through in a quartz reactor, with 100 mg of fresh catalyst and using H_2–Ar (1.55% H_2) as reducing gas. The temperature range was between 30 to 550°C, under a heating rate of 20°C min^{-1} at a flow rate of 30 cm^3 min^{-1}. The hydrogen consumption was evaluated by thermoconductivity detector.

Results and discussion

XRD patterns for the NaY, HY and Ni*/HY samples showed all the characteristic peaks of FAU structure closely as it has been reported in [14]. In these samples the FAU structure was characterized by intense reflections at 2θ=6.39° (111), 23.71° (533) and 15.76° (331). A small continuous shift to lower 2θ angles was observed when sodium was replaced by hydrogen, indicating an increase of the lattice parameters due to differences in the ionic radii of Na^+ compared to H^+. Upon modification of HY sample by conventional impregnation of nickel salt, the relative intensity of the characteristic peaks was changed without any shift in the respective peak positions indicating that nickel species are in the cavities and/or surface of HY sample (catalyst supported). The presence of nickel oxide phases along with HY phase could not be observed because of its small amount on zeolite. The main characteristics of the Y samples are shown in Table 1. IR spectra of the NaY and HY show absorption bands at 1150, 722 and 505–455 cm^{-1} due to the bonds of the internal tetrahedron structure and at 1020, 791, 573 and 380 cm^{-1} due to the external linkages of the zeolite structure. The spectra of the Ni*/HY sample are very similar to the HY which indicated that the treatment of impregnation of the nickel species on the HY zeolite does not influence the zeolite structure. BET and micropore surface areas obtained from the N_2-adsorption/desorption isotherms of the zeolite samples are summarized in Table 1. The obtained data revealed that the synthesis of the bifunctional catalyst was accompanied by a decrease in the BET surface area due to a decrease of the micropore area. This effect may be attributed to the presence of metallic oxides and extra framework aluminum species in the interior of the zeolites pores and channels.

Thermal analysis is a useful tool to provide information about the dehydratation and dehydroxylation temperatures of zeolites and also about the thermal stability of the zeolite framework. Typical TG/DTG curves of the NaY, HY and Ni*/HY zeolite samples are shown in Fig. 1. TG/DTG curves of all samples showed basically two mass loss events. The first is attributed to release of water molecules from the large cavities of zeolite and the second one can be assigned to dehydroxylation. The dehydratation and dehydroxylation process of all zeolite samples can be followed on DTA curves (Fig. 2) by two endothermic peaks between 150–160 and 700–710°C, respectively. The exothermic peak showed between 1120–1130°C in all DTA curves was attributed the lattice destruction of these samples. The obtained TG/DTA curves of all zeolites samples are in a strong agreement with the findings for similar zeolites in [15–17].

The acid properties of HY and Ni*/HY samples were evaluated by *n*-butylamine thermodesorption. Acid site density per grams of zeolite was correlated with site strength (weak, medium or strong) which is generally attributed in accordance with temperature range of *n*-butylamine desorption [7, 8]. Figure 3

Table 2 Temperature range (ΔT) and acid site density (δ) of HY and Ni*/HY zeolite samples

Samples	Weak sites		Medium+strong sites		Total
	ΔT/°C	δ/mmol g_{cat}^{-1}	ΔT/°C	δ/mmol g_{cat}^{-1}	
HY	75–262	1.230	262–804	2.114	3.345
Ni*/HY	103–302	1.423	302–802	0.904	2.327

shows TG/DTG curves of *n*-butylamine desorption of HY and Ni*/HY samples. It was possible to observe in all cases typically two larger mass changes: (*i*) 70–300°C attributed to elimination of *n*-butylamine adsorbed on the weak acid sites and (*ii*) 300–550°C attributed to elimination of *n*-butylamine adsorbed on the medium and strong acid sites. The obtained TG/DTG thermodesorption curves of all zeolites samples are in a good agreement with the reported ones for other similar zeolites [7, 18]. Kulkarni *et al*. [7] studied the *n*-butylamine thermodesorption in FeHNaY samples and detected the desorbed products by mass spectrometry as butane and ammonia. Table 2 shows the temperature range and acid site density of HY and Ni*/HY samples. In accordance with these results it was observed that for Ni*/HY zeolite the experimental

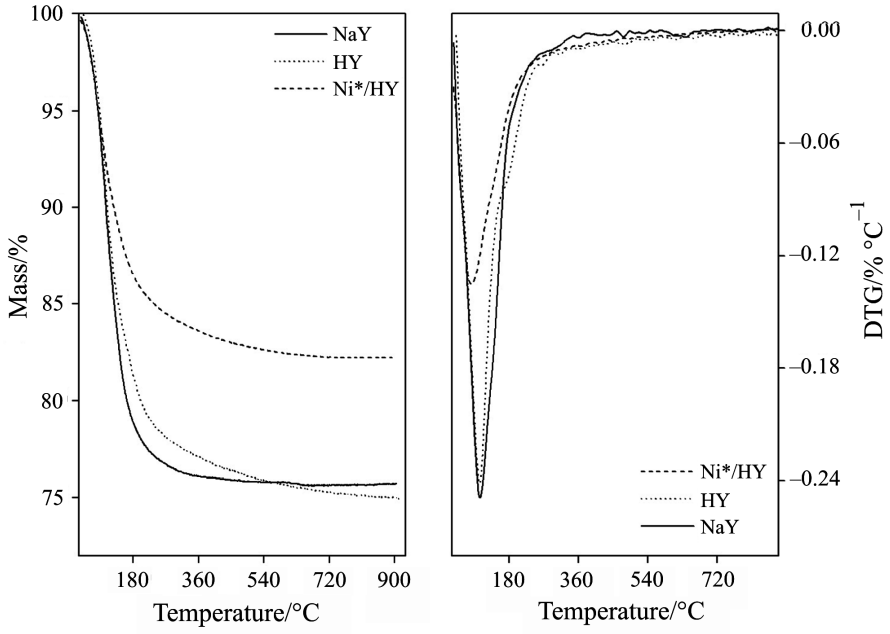

Fig. 1 TG (left) and DTG (right) curves of NaY, HY and Ni*/HY zeolites

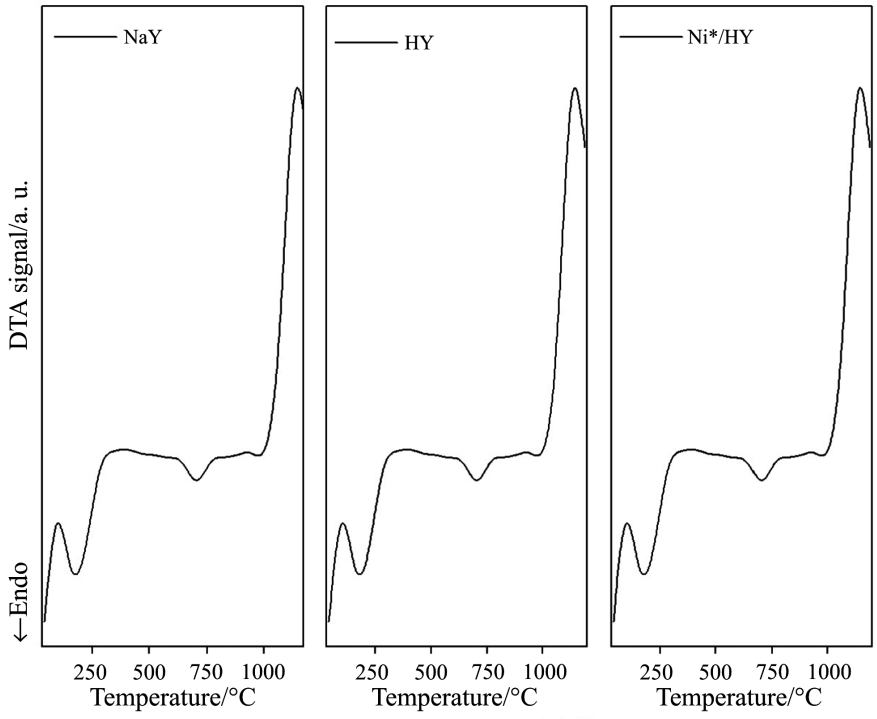

Fig. 2 DTA curves of NaY, HY and Ni*/HY zeolites

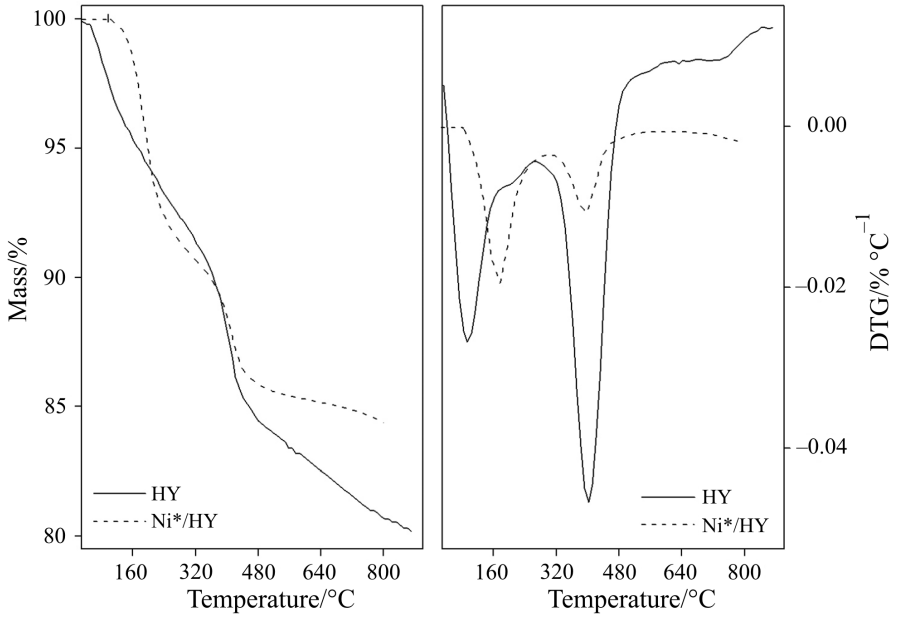

Fig. 3 TG (left) and DTG (right) curves of *n*-butylamine desorption on HY and Ni*/HY zeolites

density of strong acid sites is lower than in the case of HY zeolite. This decrease in the *n*-butylamine adsorption capacity is due to the partial blocking effect of the Ni*/HY pore system which is the result of presence of nickel oxide particles. This partial blocked pore system was caused for the dealuminization process during the calcinations, which result in a small decrease in the acid site density.

The profile of the nickel reduction on Ni*/HY sample was evaluated by temperature programmed reduction and the results are given in Fig. 4. The Ni*/HY zeolite showed two peaks for nickel reduction which appear at 238 and 507°C. These different temperatures for reduction of Ni^{2+} are related with the localization of cations in the zeolite. According to Afzal *et al*. [10] reduction peaks at lower temperatures are attributed to the reduction of the Ni^{2+} localized in the supercage and/or sodalite cavities while that at high temperatures are attributed to nickel reduction localized in hexagonal cavities; hence, it was assumed that in TPR profile showed in Fig. 4, the peaks are attributed to nickel reduction localized in the sodalite and hexagonal cavities, respectively, where the total reaction can be written as:

$$NiO+H_2 \rightarrow Ni^0+H_2O$$

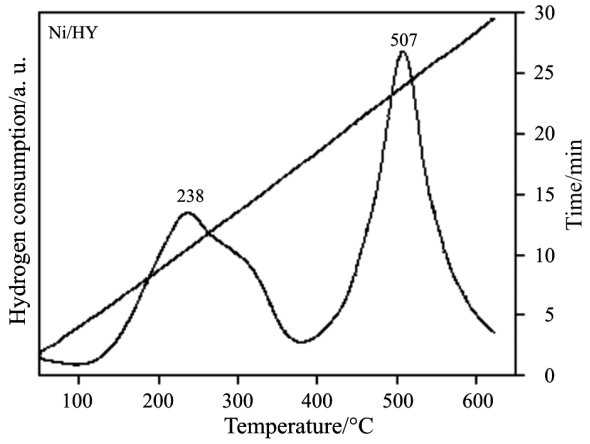

Fig. 4 TPR profile of Ni*/HY zeolite

Conclusions

XRD and FTIR analyses indicated that HY and Ni*/HY zeolites still have a similar structure to NaY zeolite. Both ion exchange and impregnation decreased the BET surface area and micropore area due to the reduction in the accessibility to micropores. The dehydration and dehydroxylation temperatures of the samples were determined from TG/DTG and were confirmed by DTA analysis. TG/DTG curves of *n*-butylamine desorption showed two mass loss events. One is for loss of *n*-butylamine adsorbed on the weak, and the other one is for the loss of *n*-butylamine adsorbed on the medium-strong acidic sites. The impregnation of nickel salt took a random distribution of the nickel oxide over HY supporter and metal reduction started at approximately 238°C.

Acknowledgements

The authors acknowledge the Agência Nacional do Petróleo (MCT/MME/PRH/ANP-30 and 14) financial support.

References

1 K. Tanabe and W. F. Hölderich, Appl. Catal. A: Gen., 181 (1999) 399.
2 A. Lugstein, A. Jentys and H. Vinek, Appl. Catal. A: Gen., 176 (1999) 119.
3 H. Yasuda, T. Sato and Y. Yoshimura, Catal. Today, 50 (1999) 63.
4 A. Chica, A. Corma and P. J. Miguel, Catal. Today, 65 (2001) 101.
5 Z. B. Wang, T. Yashima, T. Komatsu, A. Kamo and T. Yoneda, Appl. Catal. A Gen., 159 (1997) 119.
6 J. Weitkamp, Solid State Ionics, 131 (2000) 175.
7 S. J. Kulkarni and C. V. Kavedia, Thermochim. Acta, 246 (1994) 71.
8 A. O. S. Silva, M. J. B. Souza, J. M. F. B. Aquino, V. J. Fernandes Jr. and A. S. Araujo, J. Therm. Anal. Cal., 75 (2004) 699.
9 R. R. C. Pinto, M. L. M. Valle and E. F. Sousa-Aguiar, J. Therm. Anal. Cal., 67 (2002) 439.
10 M. Afzal, G. Yasmeen, M. Saleem and J. Afzal, J. Therm. Anal. Cal., 62 (2000) 277.
11 G. C. Bond and S. P. Sarsam, Appl. Catal., 38 (1988) 365.
12 Z. Zhang and W. M. H. Sachther, Advance Catal., 39 (1993) 129.
13 V. M. Rakic, V. T. Dondur, R. V. Hercigonja and V. Andric, J. Therm. Anal. Cal., 72 (2003) 761.
14 W. M. Meier, D. H. Olson and C. Baerlocher, Zeolite structure types, Elsevier, New York 1996.
15 U. D. Joshi, P. N. Joshi, S. S. Tamhankar, V. P. Joshi, B. B. Idage, V. V. Joshi and V. P. Shiralkar, Thermochim. Acta, 387 (2002) 121.
16 M. Afzal, G. Yasmeen, M. Saleem, P. K. Butt, A. K. Khattak and J. Afzal, J. Therm. Anal. Cal., 62 (2000) 721.
17 A. Dyer, Thermochim. Acta, 110 (1987) 521.
18 A. K. Ghosh and G. Curthoys, J. Phys. Chem., 88 (1984) 1130.